

Supplementary Information

Is superhydrophobicity equal to underwater superoleophilicity: hydrophilic wetting defects on superhydrophobic matrix with switchable superdewetting in both air and water

Yihan Sun ^{a,c}, Jinxia Huang ^{a*}, Zhiguang Guo ^{a,b,*} and Weimin Liu^a

^a State Key Laboratory of Solid Lubrication, Lanzhou Institute of Chemical Physics, Chinese Academy of Sciences, Lanzhou 730000, People's Republic of China

^b Ministry of Education Key Laboratory for the Green Preparation and Application of Functional Materials, Hubei University, Wuhan 430062, People's Republic of China

^c University of Chinese Academy of Sciences, Beijing 100049, People's Republic of China

* Corresponding author.

E-mail addresses: zguo@licp.cas.cn (Z. Guo) and huangjx@licp.cas.cn (J. Huang)

EXPERIMENTAL SECTIONS

Materials

Tetrabutyl titanate ($\text{Ti}(\text{OBU})_4$) was of analytical reagent (AR) grade and was purchased from Chron Chemicals Co., Ltd, ChengDu, China. Capric acid (98%, chemical pure (CP)) and trichloro (1H, 1H, 2H, 2H-perfluorooctyl) silane (97%) were obtained from Shanghai Macklin Biochemical Co., Ltd and Sigma-Aldrich, respectively. Silicon dioxide nanoparticles (99.5 %) with 15 nm average diameters were purchased from Meryer Chemical Technology Co., Ltd. Tween 80 (CP grade, MW \approx 1310) was obtained from Xilong Chemicals. Other chemical reagents were of AR grade and were directly used without any further purification. Common substrates including stainless-steel mesh (SSM), cotton fabric, copper sheet, glass slides and alumina ceramic sheet were commercially available. Deionized ultrapure water with resistivity about 18.2 M Ω cm⁻¹ was used in the whole experiment process.

Preparing of the as-prepared coating on various substrates.

Before conducting experiment, all the used vessels required to be totally clean and dry. For suspension A, 0.5 g $\text{Ti}(\text{OBU})_4$ was completely dissolved into 15 ml anhydrous ethanol, then 0.5 g capric acid was added into the above ethanol solutions under ultrasonic treatment. After introducing 5 ml 0.1 M hydrochloric acid aqueous solution, the mixtures were immediately changed to a white suspension. Then the white suspension was magnetically stirring for 10 h. 0.5 g silica nanoparticles were then added under vigorous stirring. For suspension B, 0.3 g silica nanoparticles were homogeneously dispersed into 10 ml anhydrous ethanol containing 200 μL trichloro (1H, 1H, 2H, 2H-perfluorooctyl) silane under magnetically stirring. After 10 h, suspension A and B were homogeneously mixed to obtain the final spraying inks. Afterwards, the spraying inks were loaded into a spraying gun (Mingzhi W-71, Japan), and then sprayed onto the common substrates in a line-to-line fashion with 90 PSI compressed air at a distance of 25 cm. Then, the coatings on various substrates were completely dried in ambient temperature for 3 h.

Oil-water separation test and preparing of various types of oil-in-water emulsions.

The coated fabric was used to separate immiscible light oil-water mixtures (50 %, v / v), in which the used light oils are hexane, isooctane and gasoline. The separating fluxes were determined by measuring the required time for the water layer completely permeating through the fabric surface. For preparing emulsions, oils (1,2-dichloroethane, hexane and isooctane) were mixed with water at volume ratio of 1:100, respectively. For the sake of obtaining stable emulsions, 0.2 g /L Tween 80 surfactant was then added under vigorously stirring for at least 6 h. The coated SSM with small pore sizes was used to separate three surfactant-stabilized oil-in-water emulsions and the whole separation process was only driven by gravity. The emulsion separating fluxes were calculated by measuring the collected filtrate volumes per unit time. The calculating equation was: $\text{flux} = V / St$, where V is the

collected filtrate volumes, S is the actual area of the coated SSM and t is the collecting time (5 min). The heights of feed emulsions onto the separating membrane in emulsion separation test were adjusted to 10 cm to maintain the steady driven forces.

Adhesion force test.

The adhesive force -distance curves were obtained using a high-sensitivity micro-electromechanical balance system (DCT 11 DataPhysics, Germany). The tested samples were first horizontally placed on the balance table. A 5 μL probe liquid droplet was dripped and suspended on a metal ring using a micro-syringe. The metal ring was connected by a cantilever that was linked to the balance. The force of the microbalance system was initialized to zero and the sample stage was adjusted to a suitable position to guarantee the hung droplets to touch the sample surface. Then, the metal ring with liquid droplets moved downwards with a constant speed 0.01 mm/s until the liquid droplets contact with sample surface. Afterward, the metal ring was lifted up at the same speed. The adhesive force-distance curves of the whole process were automatically recorded using a software. The peak data of the curves was recorded as the maximum adhesion force. The measuring process was repeated three times, and three adhesive force-distance curves on different positions on samples were recorded.

Instruments and Characterization.

The surface micro- / nanoarchitectures of the samples were observed using a field emission scanning electron microscope (FESEM, FEG QUANTA 650, FEI) at 30 kv accelerated voltage. The topographies of the generated nano-crosslinkers were observed using a TEM (Tecnai G2 TF20, FEI). Energy dispersive spectroscopy (EDS, EDAX) equipment attached to FESEM was performed to capture the element distributing mapping images. The static contact angles and sliding angles were measured at three different positions on the samples using a JC2000D measuring system (Shanghai Zhongchen digital instrument Co., Ltd). All the volumes of the used probe liquids (including water, hexane, gasoline, 1,2-dichloroethane, isooctane) were 5 μL . X-ray photoelectron spectroscopy (XPS, Thermo Scientific ESCALAB 250Xi) was used to investigate the fine chemical components of the samples outside. The 3D profiles and surface roughness were obtained using a 3D profiler (MicroXAM-800 Non-contact optical profilometer). All the optical photographs were taken by using a digital camera (Canon, Japan). The contents of the organics in the filtrates were determined by measuring COD values (HACH, DRB 200). FTIR spectra were recorded on a Bruker Vertex 70 instrument at attenuated total reflectance mode to investigate the chemical functional moieties of the coated fabric and pristine fabric. The fluorescence images of the samples, and optical photographs of the emulsion droplets in the emulsions and filtrates (if have) were captured by an OLYMPUS BX51 microscope (OLYMPUS GmbH, Japan). For obtaining clear fluorescence images, the samples were immersed into 0.02 mg / ml Rhodamine 6G aqueous solution for 60 s. The exposure times for obtaining fluorescence images were all adjusted to 50 ms.

The size of the feed emulsions and the filtrates were studied using dynamic light scattering (DLS) analysis recorded by Zetasizer Nano ZS (Malvern 3600, U.K.).

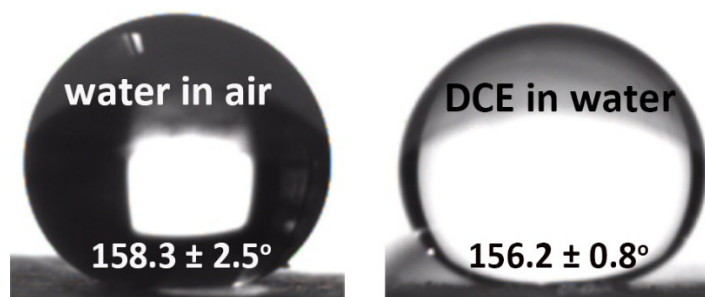


Figure S1. In-air water and underwater DCE contact angles on the dual superlyophobic SSM surface after aging at 80 °C for 2 days.

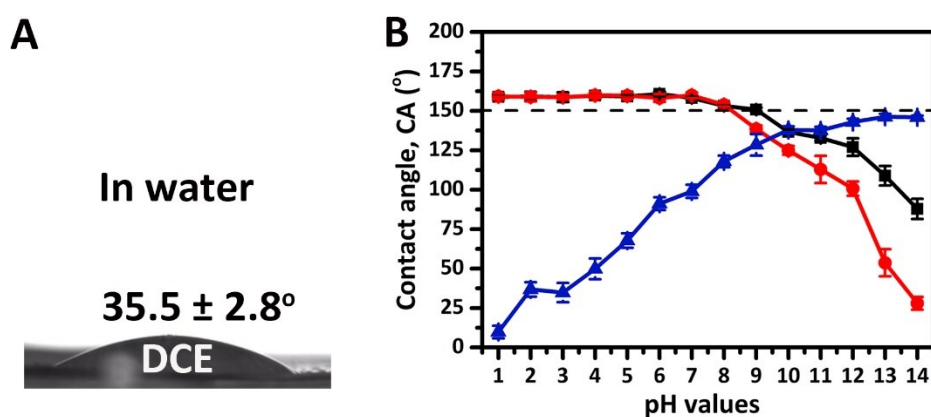


Figure S2. Superwetting behaviors on the coating fabricated by spraying Suspension A. A) Underwater DCE contact angle on the pristine coating. B) Contact angle variation of in-air water droplet with varying pH values on pristine coating (black curve), in-air water droplet (blue curve) and underwater 1,2-dichloroethane (DCE) droplet (red curve) on the coating after incubation in different corrosive aqueous solutions with varying pH values.

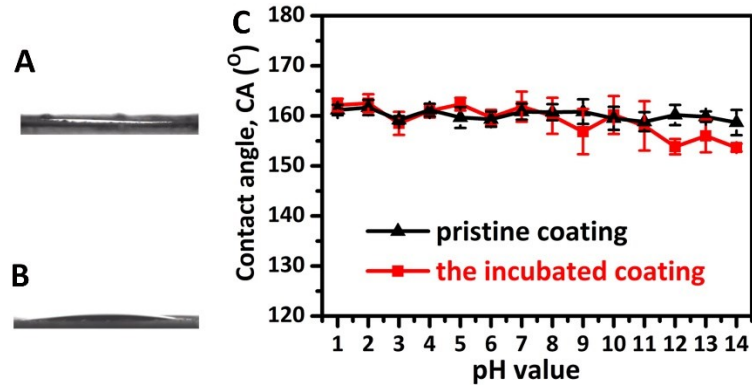


Figure S3. Superwetting behaviors on the coating fabricated by spraying Suspension B. A, B) Underwater superoleophilicity can be observed on the pristine and the coating after incubation in pH=14 strongly alkaline aqueous media. C) Contact angle variation of in-air water droplet with varying pH values on pristine coating (black curve), and in-air water droplets on the coating after incubation in different corrosive aqueous solutions with varying pH values (red curve).

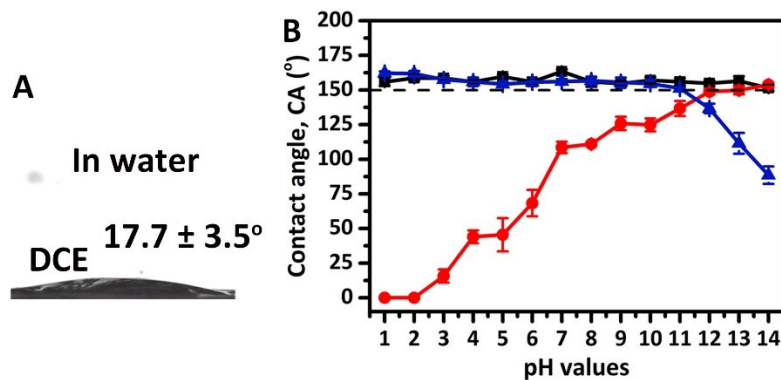


Figure S4. Superwetting behaviors on the coating fabricated by one-pot final inks. Contact angle variation of in-air water droplet with varying pH values on pristine coating (black curve), and in-air water (red curve) and underwater 1,2-dichloroethane (DCE) droplets on the coating after incubation in different corrosive aqueous solutions with varying pH values (blue curve).

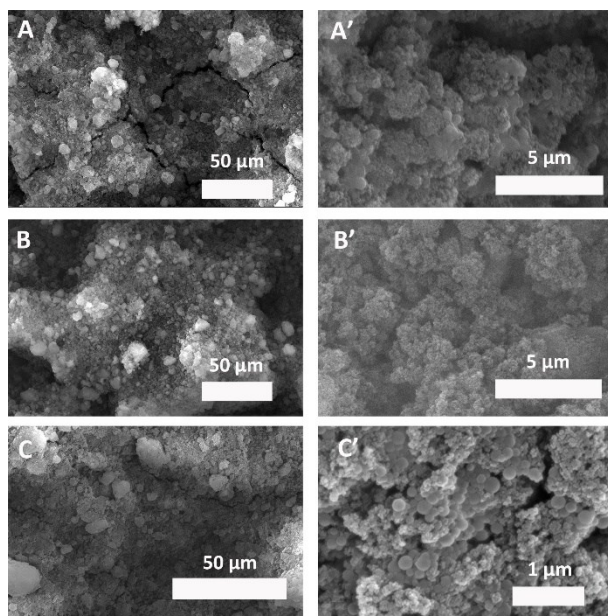


Figure S5. SEM images of the coated copper sheet obtained by being sprayed Suspension A (A, A'), Suspension B (B, B) and one-pot spraying inks (C, C').

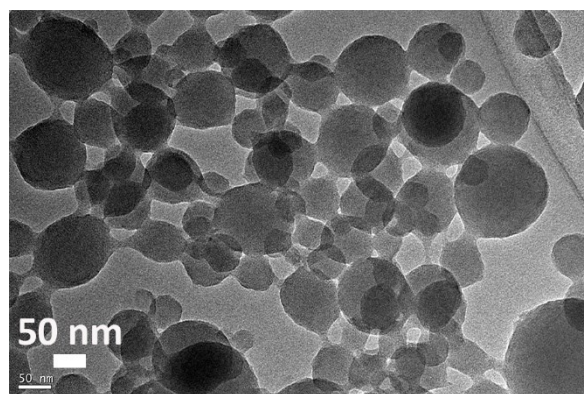


Figure S6. TEM images of the generated TiO₂ nanospheres in suspension A.

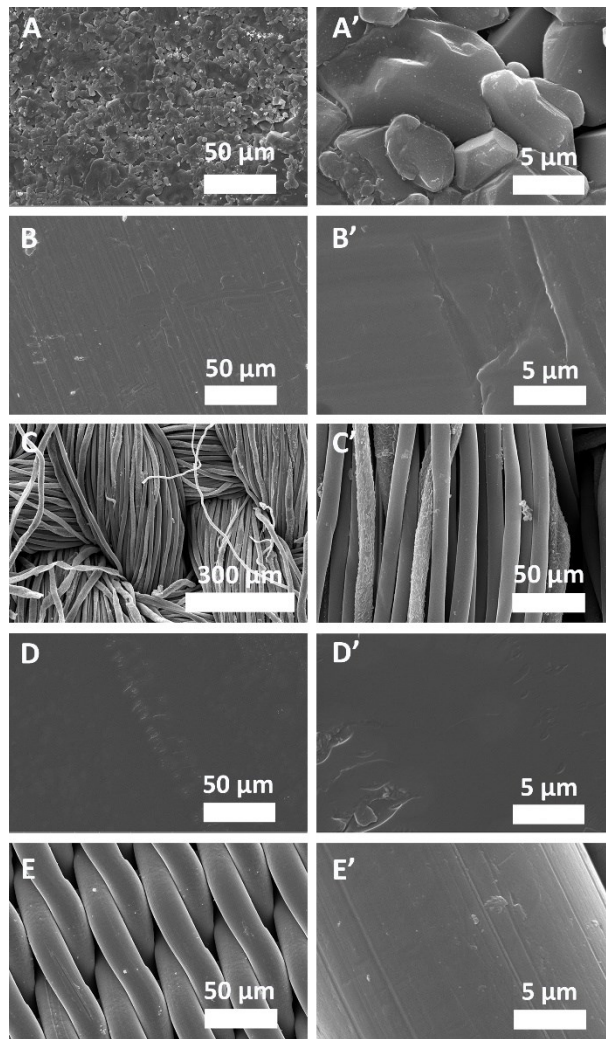


Figure S7. SEM images of the used common substrates, including aluminium oxide ceramic sheet (A, A'), copper sheet (B, B'), cotton fabric (C, C'), glass slide (D, D') and stainless-steel mesh (SSM, E, E').

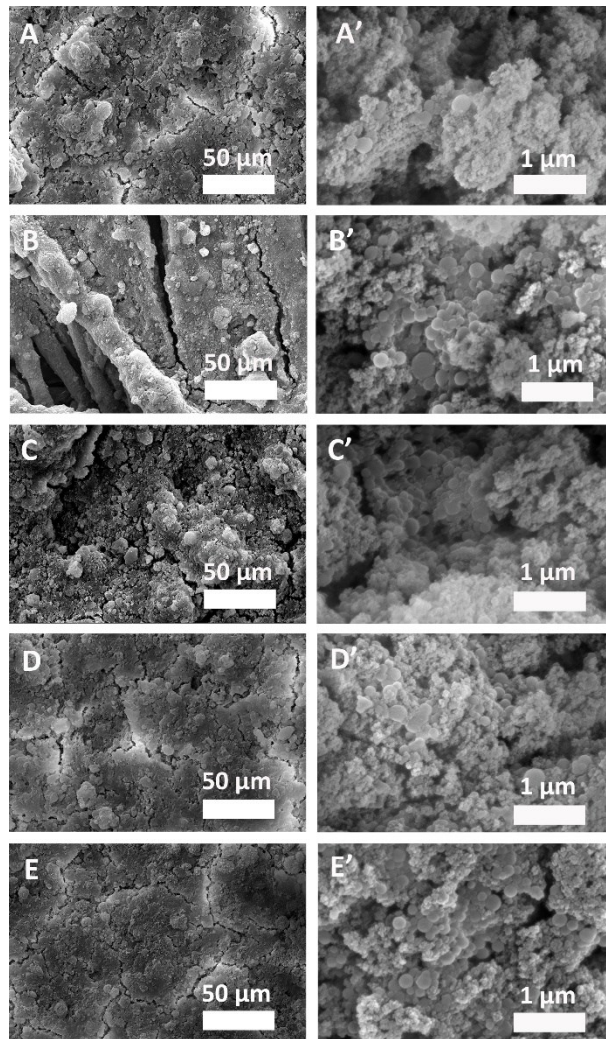


Figure S8. SEM images of the coatings on aluminium oxide ceramic sheet (A, A'), cotton fabric (B, B'), stainless-steel mesh (SSM, C, C'), glass slide (D, D') and copper sheet (E, E').

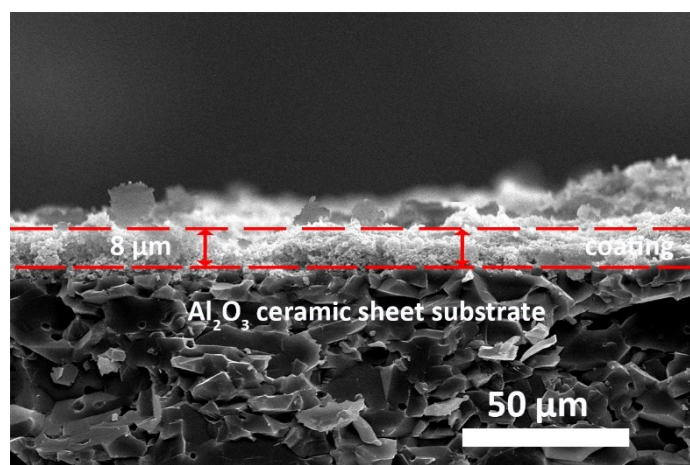


Figure S9. SEM cross-section view images for the coatings on aluminium oxide ceramic sheet. The thickness of the coating is about 8 μm.

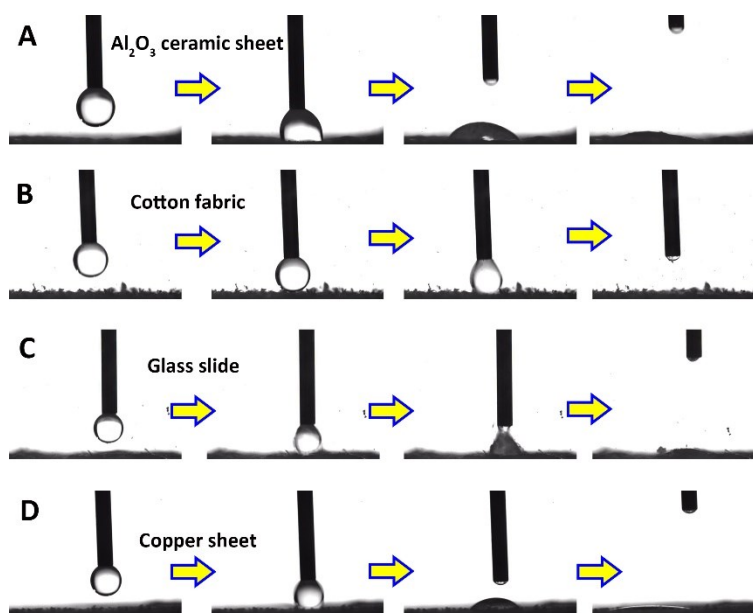


Figure S10. The underwater spreading process of oil (1,2-dichloroethane) droplets on the pristine coated ceramic sheet (A), cotton fabric (B), glass slide (C) and copper sheet (D).

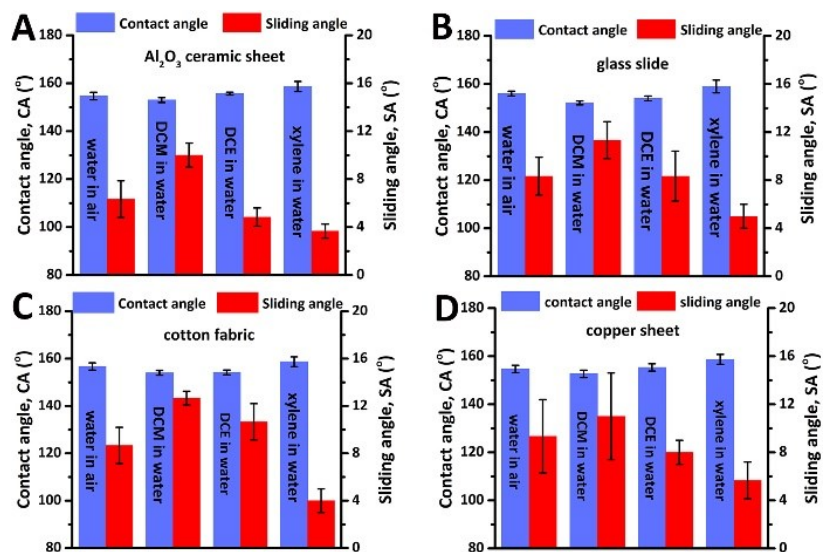


Figure S11. Superwetting properties of the coating on various substrates, including Al₂O₃ ceramic sheet (A), glass slide (B), cotton fabric (C) and copper sheet (D).

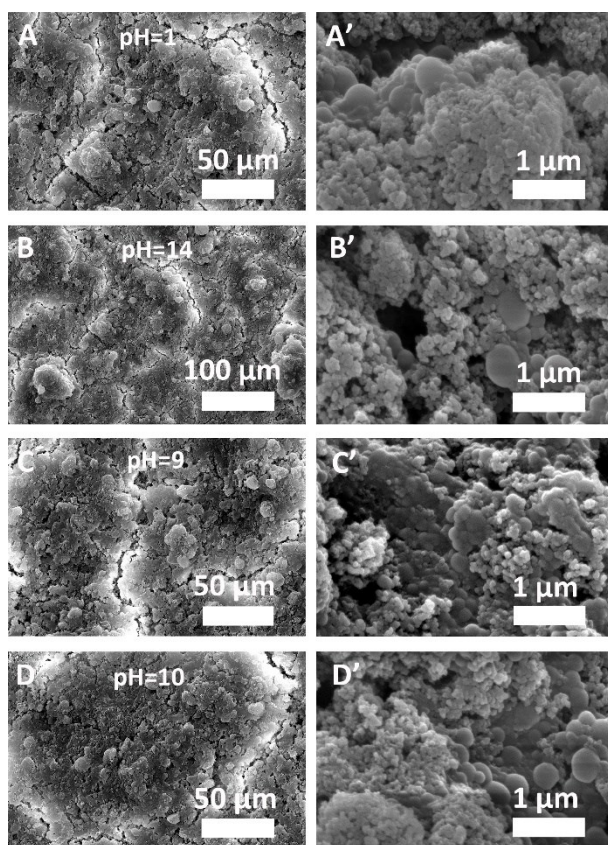


Figure S12. Surface topography variations of the coated copper sheet after soaking into pH=1 (A, A'), pH=14 (B, B'), pH=9 (C, C') and pH=10 (D, D') aqueous solution for 2 h.

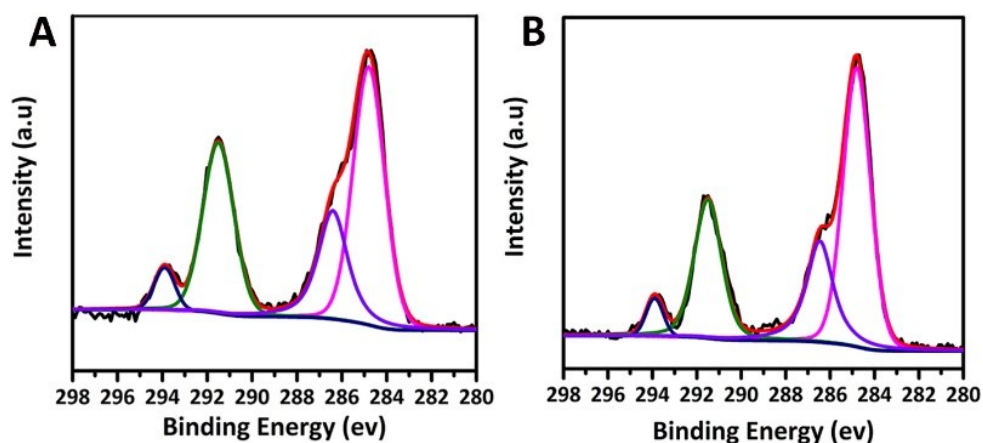


Figure S13. C 1s high-resolution XPS spectra of the pristine coated SSM (A) and the coated SSM after soaking in pH=2 acid aqueous environment (B).

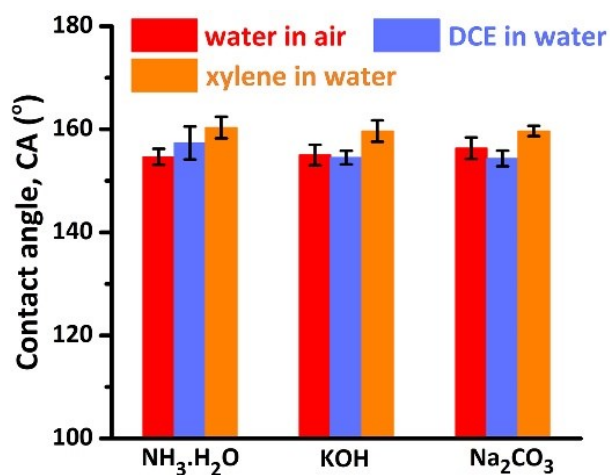


Figure S14. After being subjected to pH=10 ammonium hydroxide (NH₃.H₂O), potassium hydroxide (KOH) and sodium carbonate (Na₂CO₃) aqueous solution, the treated coating on SSM still displays dual superlyophobicity.

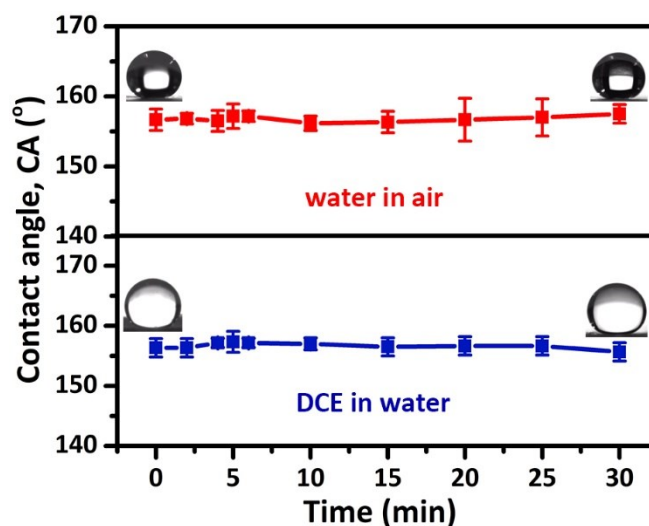


Figure S15. In-air water and underwater DCE contact angle evolution on the glass slide surface after incubation in pH=10 alkaline corrosive medium with prolonged exposing time in air. Insets display the corresponding shape profiles of water and DCE droplets on the treated sample surface in air and aqueous environment, respectively.

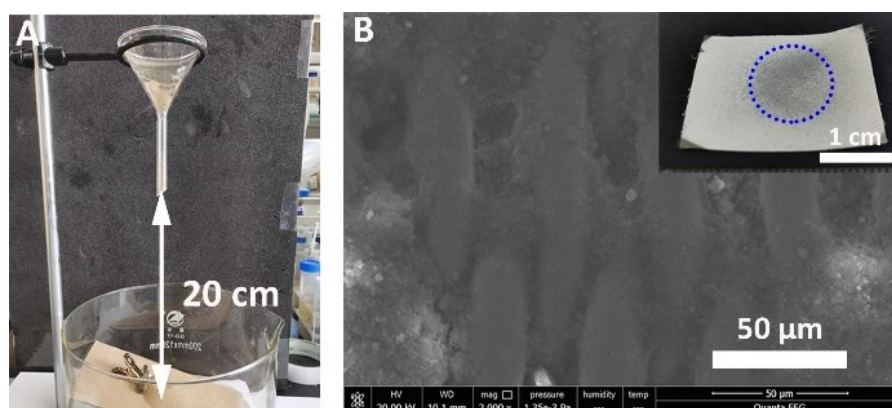


Figure S16. A) Photographs of the typical sand impact test. B) SEM image of the coated SSM. after 20 sand impact test cycles. The inset is the digital photography of the SSM. The circle (blue dash line) shows the damaged place.

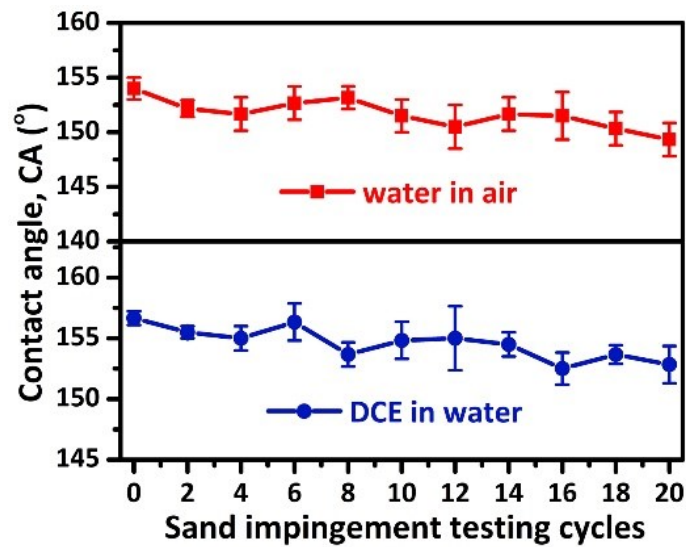


Figure S17. Contact angle variations of water droplets in air and DCE oil drops in water on the dual superlyophobic SSM surface with increasing sand impingement testing cycles.

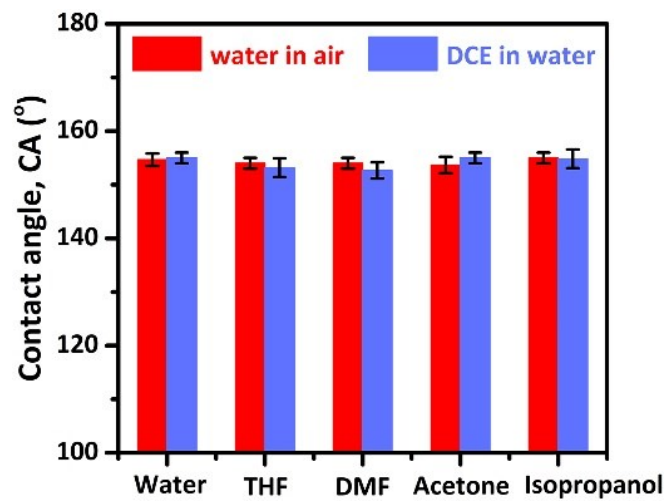


Figure S18. Contact angle variations of water droplets in air and DCE oil drops in water on the dual superlyophobic Al₂O₃ ceramic surface after 7-days submersion in water, tetrahydrofuran (THF), N, N-dimethylformamide (DMF), acetone and isopropanol, respectively.